CHEMISTRY
A EUROPEAN JOURNAL

DOI: 10.1002/chem.200801032

In Vitro Anticancer Activity and Biologically Relevant Metabolization of Organometallic Ruthenium Complexes with Carbohydrate-Based Ligands

Isabella Berger,[a] Muhammad Hanif,[a] Alexey A. Nazarov,*[a, b] Christian G. Hartinger,*[a, b] Roland O. John,[a] Maxim L. Kuznetsov,[c] Michael Groessl,[a] Frederic Schmitt,[d] Olivier Zava,[d] Florian Biba,[a] Vladimir B. Arion,[a] Markus Galanski,[a] Michael A. Jakupec,[a] Lucienne Juillerat-Jeanneret,[d] Paul J. Dyson,[b] and Bernhard K. Keppler[a]

Dedicated to Professor Jan Reedijk on the occasion of his 65th birthday

Abstract: The synthesis and in vitro anticancer activity of dihalogenido(η^6-*p*-cymene)(3,5,6-bicyclophosphite-α-D-glucofuranoside)ruthenium(II) complexes are described. The compounds were characterized by NMR spectroscopy and ESI mass spectrometry, and the molecular structures of dichlorido-, dibromido- and diiodido(η^6-*p*-cymene)(3,5,6-bicyclophosphite-1,2-*O*-isopropylidene-α-D-glucofuranoside)-ruthenium(II) were determined by X-ray diffraction analysis. The complexes were shown to undergo aquation of the first halido ligand in aqueous solution, followed by hydrolysis of a P–O bond of the phosphite ligand, and finally formation of dinuclear species. The hydrolysis mechanism was confirmed by DFT calculations. The aquation of the complexes was markedly suppressed in 100 mM NaCl solution, and notably only very slow hydrolysis of the P–O bond was observed. The complexes showed affinity towards albumin and transferrin and monoadduct formation with 9-ethylguanine. In vitro studies revealed that the 3,5,6-bicyclophosphite-1,2-*O*-cyclohexylidene-α-D-glucofuranoside complex is the most cytotoxic compound in human cancer cell lines (IC_{50} values from 30 to 300 μM depending on the cell line).

Keywords: bioinorganic chemistry · cancer chemotherapeutics · drug design · P ligands · ruthenium

Introduction

Organometallic compounds were long regarded as being synonymous with toxicity. However, in the last 20 years organometallic compounds have become increasingly important as drug entities in their own right.[1–3] In parallel to the progress made with coordination compounds after the serendipitous discovery of cisplatin as antitumor agent,[4] structurally similar organometallic compounds were considered of interest and some of them, for example, titanocene dichloride (Figure 1), underwent clinical trials.[5]

With the increasing interest in ruthenium complexes as anticancer agents, highlighted by two Ru^{III} compounds (KP1019 and NAMI-A in Figure 1)[6–8] entering clinical trials, much effort has been made to elucidate their mode of action. Protein binding and protein-mediated transport[9–13] into the tumor as well as selective reduction to Ru^{II} species,[14] which improves the reactivity toward biological nucleophiles,[14,15] are thought to be key factors for the low toxicity of this compound class.

[a] Dr. I. Berger, M. Hanif, Dr. A. A. Nazarov, Dr. C. G. Hartinger, Dr. R. O. John, Dr. M. Groessl, F. Biba, Prof. V. B. Arion, Prof. M. Galanski, Dr. M. A. Jakupec, Prof. B. K. Keppler
Institute of Inorganic Chemistry
University of Vienna
Waehringer Str. 42, 1090 Vienna (Austria)
Fax: (+43) 1-4277-9526
E-mail: alex.nazarov@univie.ac.at
christian.hartinger@univie.ac.at

[b] Dr. A. A. Nazarov, Dr. C. G. Hartinger, Prof. P. J. Dyson
Institut des Sciences et Ingénierie Chimiques
Ecole Polytechnique Fédérale de Lausanne (EPFL)
1015 Lausanne (Switzerland)

[c] Dr. M. L. Kuznetsov
Centro de Química Estrutural
Complexo I, Instituto Superior Técnico
TU Lisbon, Av. Rovisco Pais, 1049-001 Lisbon (Portugal)

[d] F. Schmitt, Dr. O. Zava, Dr. L. Juillerat-Jeanneret
University Institute of Pathology
Centre Hospitalier Universitaire Vaudois (CHUV)
Rue du Bugnon 25, 1011 Lausanne (Switzerland)

Supporting information for this article is available on the WWW under http://dx.doi.org/10.1002/chem.200801032.

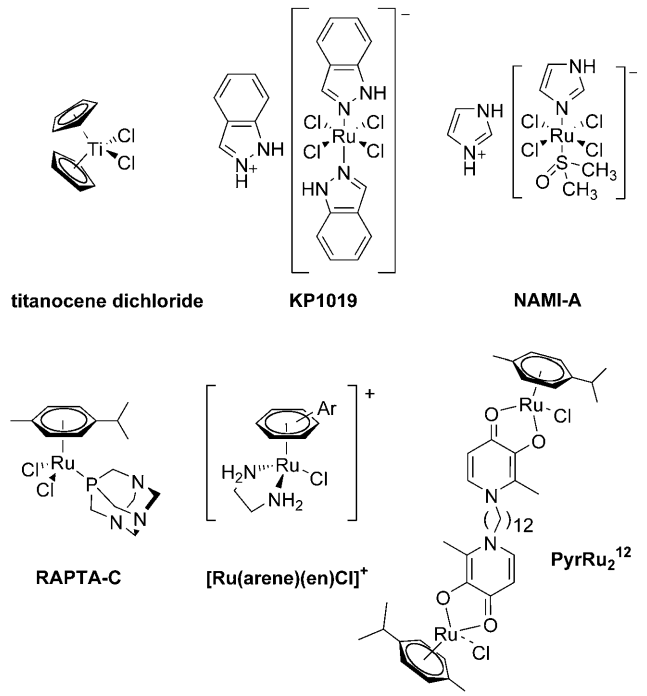

Figure 1. Structures of investigated anticancer compounds.

The chemistry of organometallic Ru^{II} compounds is well developed, and these compounds are used in many catalytic processes, for example, olefin metathesis, hydrogenation, hydroformylation, and hydrogen generation.[16–18] In recent years, the first examples of mono- and dinuclear tumor-inhibiting Ru^{II} arene complexes (Figure 1) were introduced.[19–25] The two most extensively studied approaches involve the coordination of the Ru center by 1,3,5-triaza-7-phosphaadamantane (pta) and ethylenediamine (en) ligands (Figure 1). Although the neutral pta compounds are known to exhibit selective activity in cancer cells, but not in nontumorigenic models,[26] en complexes proved to be active in cultures of wild-type and cisplatin-resistant human ovarian cancer cells.[19] Furthermore, the pta compounds were shown, similar to NAMI-A, to be active in vivo against lung metastases derived from an MCa mammary carcinoma in CBA mice.[21,26,27]

Herein we report on the synthesis and (bio)analytical characterization of RAPTA-C analogues in which the pta has been replaced by 3,5,6-bicyclophosphite-α-D-glucofuranoside ligands.[28–30] By modification of the carbohydrate moiety, the lipophilicity of the complexes can be modulated to yield coordination compounds with high aqueous solubility ideally suited for intravenous administration, or hydrophobic species that facilitate cellular uptake.[31] The compounds were characterized by different analytical methods, and the molecular structures of three complexes were determined by X-ray diffraction analysis. Furthermore, the hydrolytic behavior, the affinity to proteins and model nucleobases, and the in vitro antineoplastic activity of the complexes against human SW480 colon adenocarcinoma, CH1, A2780 and cisplatin-resistant A2780 ovarian carcinoma, A549 lung carcinoma, Me300 melanoma, LNZ308 glioblastoma, and HCEC endothelial human cell lines were determined.

Results and Discussion

Synthesis: Ru^{II} organometallic complexes **1–6** based on 3,5,6-bicyclophosphites of α-D-glucofuranoside were obtained by reaction of the dimers $[\{Ru(\eta^6\text{-}p\text{-cymene})X_2\}_2]$ (X = chlorido, iodido, bromido) and different 3,5,6-bicyclophosphites under mild conditions (Scheme 1). Complex **6** was found to be very sensitive even to gentle heating, and therefore the reaction was carried out at room temperature. Complexes **1–6** were obtained in nearly quantitative yields.

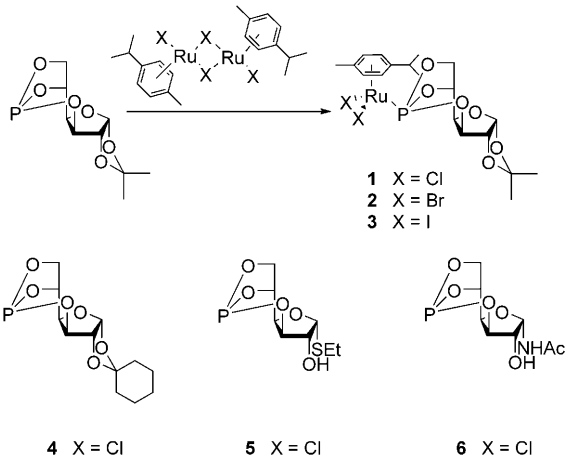

Scheme 1. General scheme for synthesis of Ru^{II} arene complexes with different 3,5,6-bicyclophosphite-α-D-glucofuranosides.

All compounds were fully characterized by 1D and 2D NMR spectroscopy. The coordination of the P-containing ligand to the Ru center resulted in a shift of the ^{31}P NMR signal from about $\delta = 119$ to about 135 ppm in the case of the chlorido and iodido complexes, while for the bromido complex a signal at about 133 ppm was observed. In the ^1H NMR spectra in $CDCl_3$ two sets of signals were observed (four doublets for the Ar-H and two doublets for the Ar-CHCH_3 protons). In contrast, in D_2O the aromatic protons and the methyl groups resulted in two doublets and one doublet, respectively. A similar situation was observed in the ^{13}C NMR spectra, and also reported previously for related complexes.[32]

Molecular structure determinations: The crystal structures of **1–3** were determined by X-ray diffraction (Figure 2). The complexes crystallize in the orthorhombic space group $P2_12_12_1$. The ruthenium(II) center adopts a piano-stool geometry with two halogenido ligands and the phosphorus atom of the bicyclophosphite ligand as the legs and the arene ligand as the seat. The distance between the ruthenium center and the centroid of the arene ring of 1.711 Å in **1**

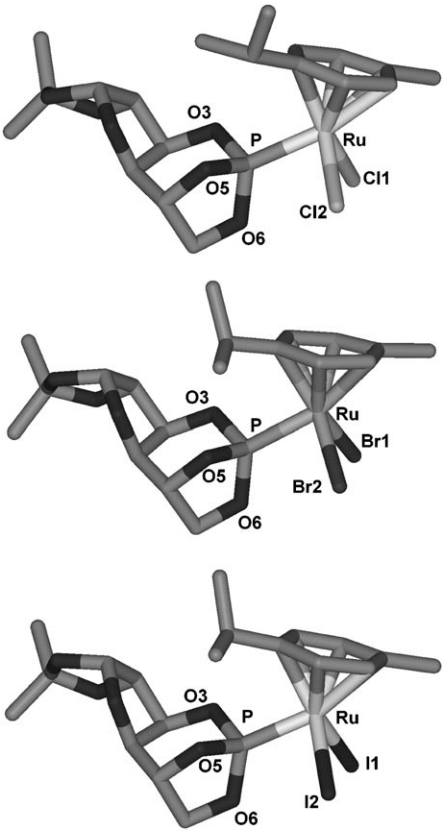

Figure 2. Molecular structures of **1** (top), **2** (middle), and **3** (bottom) showing the atom numbering schemes around the ruthenium center. Hydrogen atoms are omitted for clarity.

is similar to that of $[RuCl_2(\eta^6\text{-}p\text{-cymene})(pta)]$ (1.701[33]) and $[RuCl_2(\eta^6\text{-}p\text{-cymene})(pta\text{-}Me)]$ (1.692 Å[34]). The Ru–Cl1, Ru–Cl2, and Ru–P bond lengths in **1** (2.3886(11), 2.4098(10), 2.2406(10) Å) are comparable to those in $[RuCl_2(\eta^6\text{-}C_6Me_6)\{P(OMe)_3\}]$[35] (2.4138(9), 2.4042(9), and 2.2678(9) Å, respectively) and $[RuCl_2(\eta^6\text{-}p\text{-cymene})\{P(OPh)_3\}]$[36] (2.4022(8), 2.3992(8) and 2.2642(8) Å, respectively). While the conformations of the dioxaphospholane ring (labeled as A in Figure S1 of the Supporting Information) in both the metal-free[37] and the coordinated bicyclophosphite are practically identical, the conformations of the dioxaphosphorinane (B), furanose (C), and dioxalane (D) rings are different (see Table S1 and Figure S1 in the Supporting Information). The sums of the O–P–O and P–O–C valence angles of 301.8 and 333.9° are comparable with the corresponding values in the metal-free bicyclophosphite (297.3 and 342.6°, respectively).

The molecular structures of **2** and **3** are very similar to that of **1**, except that the Ru–Br1 and Ru–Br2 bonds (2.5387(4) and 2.5413(3) Å) as well as the Ru–I1 and Ru–I2 bonds (2.7120(5) and 2.7178(6) Å) are significantly longer than the Ru–Cl bonds in **1**. The Ru–P bond lengths (2.2357(8) and 2.2275(14) Å for **2** and **3**, respectively) are comparable to that of **1**. Exchange of the chlorido ligand by bromido or iodido does not cause significant deviations in the P–O bond lengths and conformation of the bicyclophosphite moiety. Exchange of the halido leaving group modifies the hydrolysis kinetics and the lipophilicity of the complexes, but ultimately identical hydrolysis products are formed.

Hydrolysis: The behavior of putative drug compounds in water is important for their potential clinical application. Moreover, the formation of aqua species plays a critical role in the mode of action of metal-based drugs with respect to drug activation by facilitating the reaction of the complex with the biomolecular target.[15,38,39]

Hydrolysis of **1** was studied by $^{31}P\{^1H\}$ NMR spectroscopy, UV/Vis spectroscopy, ESIMS, and DFT calculations. Immediately after dissolution UV/Vis spectra of **1** in water show absorption bands at $\lambda = 345$ and 476 nm, which both decrease with time (Figure S2 in the Supporting Information). Over 48 h a new band appears at $\lambda = 288$ nm. The same spectrum was observed after addition of two equivalents of $AgNO_3$.

To characterize the hydrolysis products (see Scheme 2 for the species formed during hydrolysis), a freshly prepared solution of **1** was studied by $^{31}P\{^1H\}$ NMR spectroscopy in water containing 10% of D_2O (Figure 3). Initially only a single peak was observed at $\delta = 136.1$ ppm. Over time several hydrolysis products were formed. It appears that initially one chlorido ligand is replaced by H_2O (Scheme 2) to form the diastereomers **1a** and accordingly two peaks of equal relative intensity in the ^{31}P NMR spectrum ($\delta = 137.1$ and 137.7 ppm). Notably, this first hydrolysis step can be reversed by addition of a tenfold excess of NaCl to a solution of **1a** to afford quantitatively **1**.

A peak assignable to the bis-aqua complex **1b** was not observed under these conditions; instead, the P–O bond of the phosphite was hydrolyzed (see below for detailed discussion), and new signals resulted at $\delta = 95.1$ and 96.0, assigned to diastereomers **1c**, and at $\delta = 95.2$ ppm (**1d**).The bis-aqua complex **1d** and the mixture of diastereomeric Cl/H_2O complexes **1c** subsequently form dimers of the proposed composition $[Ru_2(p\text{-cymene})_2(\mathbf{L^{1hyd}})_2X]^{3+}$ (X = Cl, OH) after about 24 h (based on NMR and MS data, see below), which result in signals at $\delta = 123.6$ and 122.2 ppm. The distribution of species formed during the hydrolysis process is shown in Figure S3 of the Supporting Information.

Notably, cleavage of the P–O–C5 bond in the presence of H_2O_2 or O_3 was previously reported for **L1**[40,41] and induces oxidation of the P^{III} center to P^{V}. If **L1** is coordinated to a ruthenium center, this reaction is accessible at room temperature in aqueous solution, and the oxidation state of the P atom remains unchanged.

By addition of $AgNO_3$ to **1**, both chlorido ligands were replaced and the bis-aqua species with (**1d**) and without (**1b**) hydrolyzed P–O bonds were obtained ($\delta(^{31}P) = 138.4$ and 95.2 ppm, respectively). Notably, **1d** only formed a dimer in low yield, although this step occurs much more slowly when the compound is hydrolyzed by the addition of $AgNO_3$ (Scheme 2 and Figure S4 in the Supporting Information).

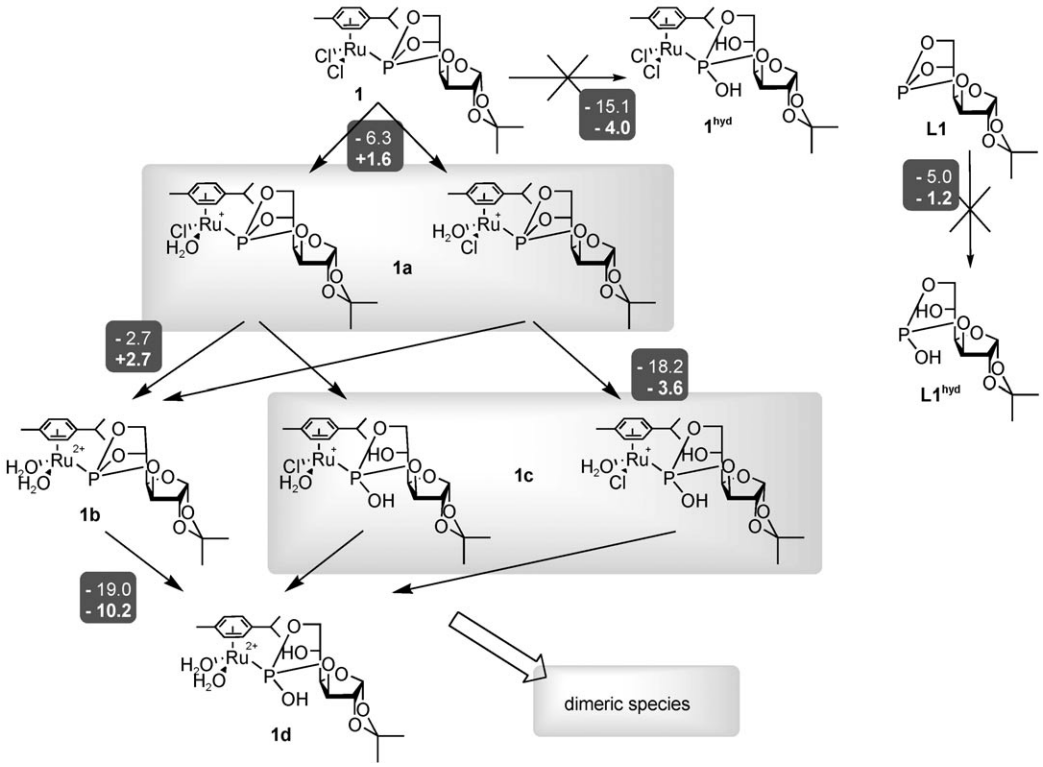

Scheme 2. Proposed hydrolysis of **1** based on experimental data and calculations. The calculated ΔH_g (plain text) and ΔH_s (bold) values for *p*-xylene model complexes are indicated.

For compounds **2**–**4** and **6** a hydrolysis behavior similar to **1** was observed in H_2O, although the aqueous solubility of **2** and **3** is limited. However, the behavior of **5** was somewhat different in terms of kinetics and hydrolysis products, most probably due to exchange of the thioethyl moiety by water.[42]

The structure of **1d** (Scheme 2) was further corroborated by 1D and 2D NMR spectroscopy. As observed by $^{31}P\{^1H\}$ NMR spectroscopy, removal of both chlorido ligands by addition of $AgNO_3$ induced rapid formation of **1d**, which was accompanied by significant changes in chemical shift in the ^1H and ^{13}C NMR spectra. In particular the H6 and H6′ signals shifted to high field from $\delta = 4.6$ and 4.2 ppm to $\delta =$ 4.0 and 3.6 ppm, while those of protons H2, H3, and H4 showed only minor changes of about $\Delta\delta = 0.05$ ppm. The most drastic change was observed for H5, which showed a shift from $\delta = 5.1$ to 4.1 ppm together with loss of coupling to the P center (Figure 4). Furthermore, in the ^{13}C NMR spectrum, C4 and C5 changed their multiplicity from doublets to singlets, again due to loss of coupling to phosphorus. All these observations indicate that hydrolysis of the P–O bond of the 3,5,6-bicyclophosphite ligand at P–O–C5 has taken place. However, all attempts to isolate the hydrolysis products and characterize them in the solid state were unsuccessful.

The formation of several species was also observed by ESIMS. The mass spectrum recorded immediately after dissolution contains signals assignable to $[M-Cl]^+$, $[M+Na]^+$, $[2M-Cl]^+$ and $[2M+Na]^+$. During the hydrolysis of **1**, species at *m*/*z* 501.2 were observed which could be assigned to different singly-charged ions and may possibly result from **1a**–**1d** (Scheme 2). Furthermore, the dimeric species $[2\mathbf{1c}-Cl-2H_2O-2H]^+$ and $[2\mathbf{1d}-3H_2O-2H]^+$ were observed with *m*/*z* 1037.1 and 1019.1, respectively.

To substantiate the experimental data, thermodynamic quantum chemical calculations on phosphite **L1** and the *p*-xylene model complexes **1′**–**1d′** were performed. The calculations indicate that substitution of the chlorido ligands with H_2O is slightly endothermic, with ΔH_s values of +1.6 and +2.7 kcal mol^{-1} for replacement of the first and second ligand, respectively. A noticeably positive ΔH_s value for the formation of **1b′** (+4.3 kcal mol^{-1} relative to **1′**) may explain the lack of experimental detection of bis-aqua complex **1b**, which is rapidly hydrolyzed to **1d**.

Hydrolysis of the free phosphite **L1** is only slightly exothermic (Scheme 2). Coordination of **L1** to the metal may facilitate hydrolysis of the phosphite due to transfer of electron density from the P atom to the metal, which increases the positive charge on the phosphorus atom. Indeed, the calculated NBO atomic charges on the P centers in **L1** and **1′** are +1.6 e and +2.1 e, respectively.

The gas-phase ΔH_g value for hydrolysis of the free ligand **L1** is −5.0, whereas the hydrolysis of complex **1′** is 10.1 kcal mol^{-1} more exothermic. However, consideration of solvent effects reduces this difference to only 2.8 kcal mol^{-1}. Thus, solvation is the main factor which levels, at least from the

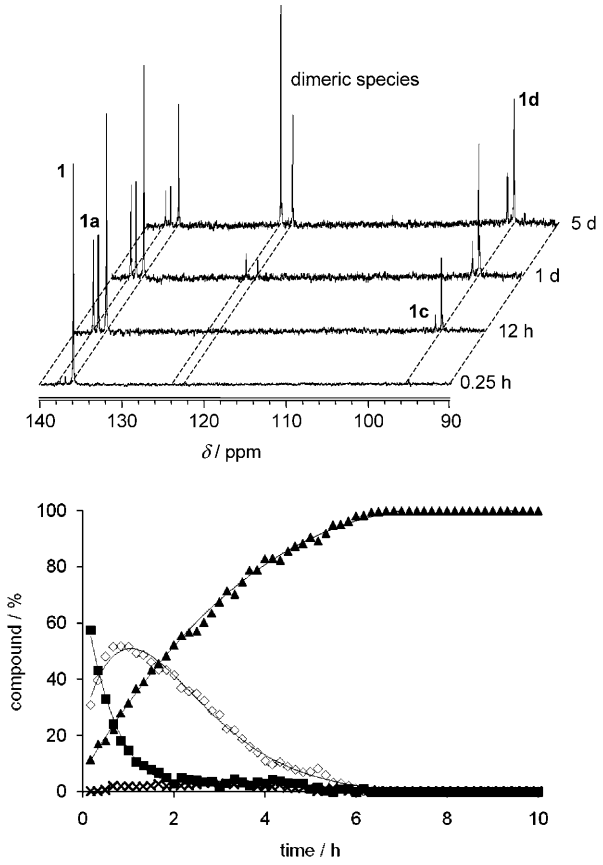

Figure 3. Top: $^{31}P\{^{1}H\}$ NMR spectra recorded during the hydrolysis of **1** in H_2O:D_2O (9:1). Bottom: distribution of species after addition of $AgNO_3$ to a solution of **1** in H_2O:D_2O (9:1) recorded over 10 h. **1**■, **1a**◇, **1b**×, **1d**▲.

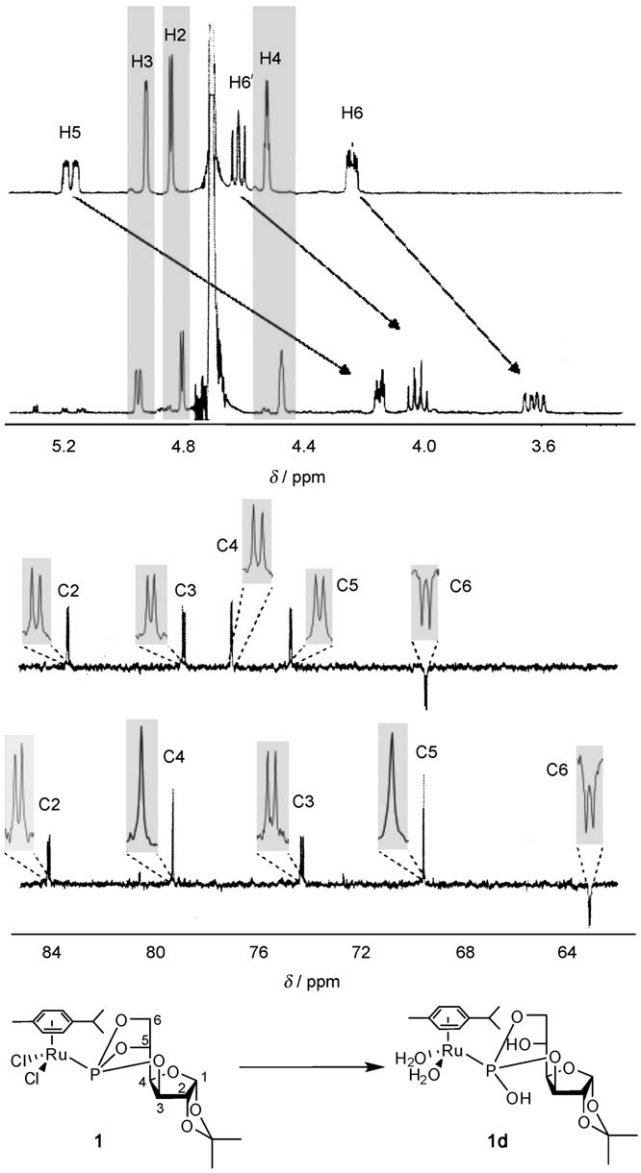

Figure 4. Characterization of the hydrolysis products derived from P–O bond cleavage in the phosphite ligand by ^{1}H (top) and ^{13}C NMR spectroscopy (middle); the top spectra were recorded immediately after dissolution in D_2O, and the spectra at the bottom after addition of $AgNO_3$ to induce complete hydrolysis of the complex.

thermodynamic viewpoint, the behavior of **L1** and **1′** towards hydrolysis. Although the detailed mechanism is unknown, it is assumed that the hydrolysis of **1** should also be hampered from the kinetic viewpoint due to steric hindrance by the Ru and O atoms during hydrolysis of the P–O bond. These inferences by the experimental findings indicate that hydrolysis does not occur for both free phosphite **L1** and complex **1**, prior to substitution of it's chlorido ligands by aqua ligands.

Hydrolysis of mono-aqua complex **1a′** is only slightly exothermic ($\Delta H_s = -3.6$ kcal mol^{-1} for the more stable diastereomer of **1a′**), but for bis-aqua complex **1b′** $\Delta H_s = -10.2$ kcal mol^{-1}. Therefore, from the thermodynamic point of view, hydrolysis of the coordinated phosphite in **1b′** is most favorable. Kinetically, hydrolysis of **1a** and **1b** is expected to be more facile than that of **1**, because in the former case the coordinated water, rather than an outer-sphere water molecule, conceivably participates in the reaction by attacking the P–O bond, and steric factors become less important. Thus, on the basis of the experimental and theoretical data the hydrolysis of **1** follows the sequence of reactions shown in Scheme 2.

To obtain information about the influence of chloride concentration and pH on the hydrolysis process, $^{31}P\{^{1}H\}$ NMR spectra of **1** were recorded in 4 and 100 mM NaCl solution. A 4 mM solution of sodium chloride did not suppress hydrolysis significantly, and the species distribution was similar to that in water. In contrast, almost no hydrolysis products were observed in 100 mM NaCl solution (see Figure S5, Supporting Information, for the dependence of hydrolysis on NaCl concentration). Furthermore, suppression of hydrolysis at the ruthenium center also inhibits hydrolysis of the P–O bond of the ligand to a large degree, that is, $\mathbf{1}^{hyd}$ is not formed under these conditions. These results were confirmed by UV/Vis spectroscopy.

Protein binding studies: The role of serum transport proteins either in delivery of drugs to their cellular targets or in deactivating metal-based anticancer drugs is of importance.[11,43–52] Therefore, the binding capabilities of the synthesized Ru compounds towards human serum albumin (HSA) and transferrin (Tf) and also towards smaller model proteins were assayed by capillary zone electrophoresis (CZE) and/or mass spectrometry.

To determine the kinetics of binding to the proteins, the decrease in the relative peak area of the Ru complexes was analyzed in phosphate buffer at pH 7.4 (Figure 5), to simulate physiological conditions. The rate constants for hydrolytic decomposition and for interactions with the biomolecules were calculated by assuming pseudo-first-order kinetics, whereas the half-lives of the compounds were determined graphically from plots of relative peak area versus time (Figure 5). Compounds **1**, **4**, and **6** showed similar rate constants for hydrolytic decomposition, while **5** was significantly more stable. Note that Ru–phosphate adducts may form in phosphate buffer, probably in addition to the hydrolysis products observed in water. However, to obtain the protein binding constants, the hydrolysis constants were determined under the same conditions.

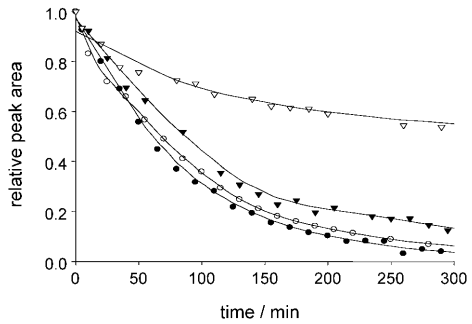

Figure 5. Comparison of the hydrolysis kinetics of **1** and **4**–**6** in 20 mM phosphate buffer (pH 7.4). **1**●, **4**○, **5**▽, **6**▼.

In contrast to hydrolysis, binding towards both human serum albumin and transferrin seems to proceed at essentially the same rate for all the investigated compounds (Table 1). Binding to albumin is kinetically favored over binding to transferrin (see Figure 6 for time-dependent electropherograms for the reaction of **6** with transferrin). This may be attributable to the greater number of (presumably) unspecific binding sites and has also been observed for other metal complexes.[13,53] Since only the linear range of ln(peak area) versus time plots can be considered for calculations of pseudo-first-order rate constants, the hypothetical extrapolation according to the linear equation used for the estimations of pseudorate can result in different half-lives, as evaluated graphically from the real curves, due to the complexity of the samples.

Table 1. Rate constants for hydrolysis of **1** and **4**–**6** and their reaction with transferrin and HSA. The correlation coefficients R^2 for the corresponding rate equation are given in parentheses. See Experimental Section for conditions.

	Hydrolysis		HSA		Tf	
	k_{hyd} [min^{-1}]	$\tau_{1/2}$ [min]	k_{bind} [min^{-1}]	$\tau_{1/2}$ [min]	k_{bind} [min^{-1}]	$\tau_{1/2}$ [min]
1	0.0117 (0.999)	61	0.0105 (0.998)	55	0.0069 (0.999)	56
4	0.0097 (0.999)	68	0.0103 (0.999)	59	0.0081 (0.997)	58
5	0.0016 (0.999)	695	0.0094 (0.997)	410	0.0092 (0.997)	175
6	0.0090 (0.998)	86	0.0116 (0.997)	50	0.0100 (0.998)	55

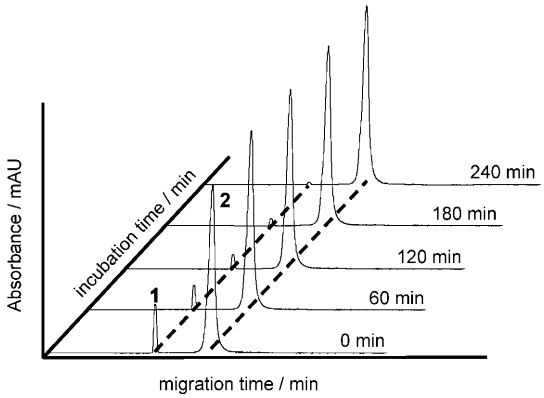

Figure 6. Monitoring the interaction of **6** with transferrin by capillary electrophoresis. Peak 1: Ru complex, peak 2: protein. For conditions, see Experimental Section.

In addition, binding of the ruthenium arene complexes toward the cellular proteins ubiquitin and cytochrome c and the plasma protein transferrin was studied by mass spectrometric methods, and **1** was chosen as representative compound for these experiments. Samples containing varying drug-to-protein ratios from 1:1 to 8:1 were studied. In the case of ubiquitin and cytochrome c, no adduct formation could be observed after 24 h of incubation at 37 °C, even with an eightfold excess of the drug. In contrast, binding to transferrin could already be observed at 1:1 ratio after 30 min. Interestingly, even at ratios of up to 8:1, only adducts assignable to the binding of two complexes were detected (Figure 7). This is in accordance with the assumption

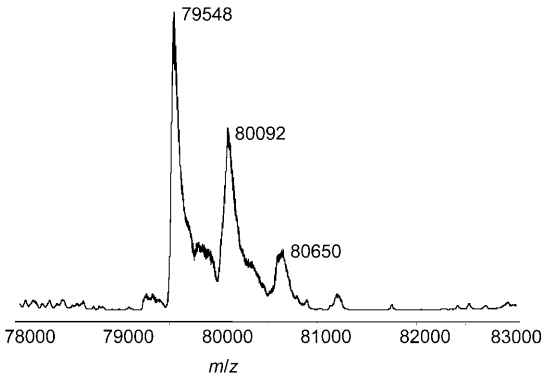

Figure 7. Deconvoluted mass spectrum of transferrin incubated with a fourfold excess of **1** in 20 mM ammonium carbonate buffer at 37 °C and pH 7.4, recorded after 30 min of incubation. The peak at m/z 79548 corresponds to the protein itself, the peak at m/z 80092 to the mono-adduct, and the signal at m/z 80650 to the bis-adduct.

of specific binding in the iron-binding pockets, which could also explain the slower binding kinetics toward transferrin in comparison to albumin. For transferrin, a molecular weight of 79548 ± 15 Da was determined, which is in good agreement with the literature.[54] The observed mass increase of approximately 540 Da could be assigned to a conjugate formed with the complex upon loss of a chlorido ligand. A mass increase of approximately 1100 Da could be attributed to formation of a bis-adduct.

Interaction with 9-ethylguanine: DNA is regarded as an important target for metal-based anticancer agents, especially for Pt complexes, and binding to nucleobases is widely studied by methods such as NMR spectroscopy and capillary electrophoresis to provide information on the mode of action.[51,55–59] Interaction of **1** with the model compound 9-ethylguanine (9EtG) was investigated under different conditions. Incubation of **1** with 9EtG at molar ratios of 1:1 and 1:2 resulted in formation of the respective 9EtG adduct by exchange of a chlorido ligand (two diastereomers at approximately 139 and 141 ppm in the ^{31}P NMR spectra; Figure 8), and secondly an adduct with the hydrolyzed P ligand (two diastereomers around 96 and 98 ppm). Addition of equimolar amounts of 9EtG to a solution of **1d** (obtained by treatment of **1** with 2 mol of $AgNO_3$) resulted in formation of a pair of signals at approximately 96 and 98 ppm, assignable to the pair of diastereomers that was also observed at an incubation ratio of Ru complex:9EtG = 1:2. No other signals appeared in the NMR spectrum even after 72 h of incubation. The finding that all hydrolysis species are able to bind to 9-ethylguanine demonstrates their potential role in vitro.

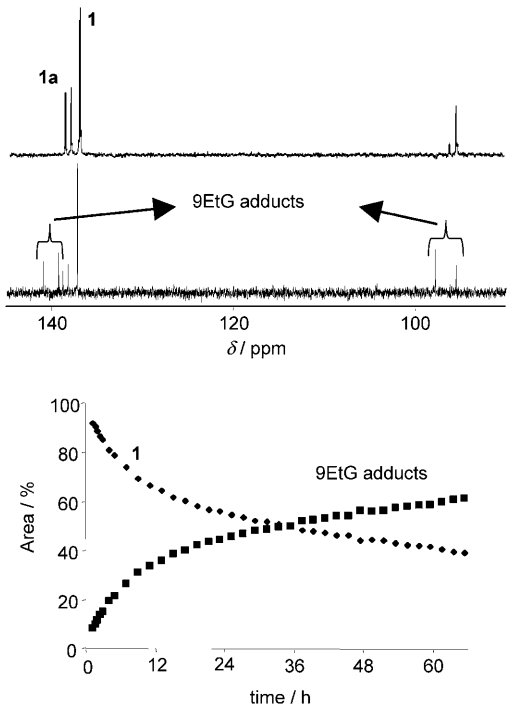

Figure 8. Top: Reaction of **1** with 9EtG studied by ^{31}P NMR spectroscopy. Bottom: percentage of adduct formed during incubation of **1** with 9EtG at 1:2 molar ratio over 65 h in D_2O.

Mass spectrometric studies of a mixture of **1** and 9EtG (1:1) after 24 h of reaction revealed, in addition to a peak assignable to unchanged 9EtG at *m/z* 180.0 $[9EtG+H]^+$, species observed during the hydrolysis studies and peaks at *m/z* 679.7, 1180.0, and 1359.0, which were assigned to $[\mathbf{1}-2Cl+OH+9EtG]^+$, $[\mathbf{1c}-2OH+9EtG-H]^+$, and $[\mathbf{1c}-2OH+29EtG-H]^+$, respectively.

Note that neither ESIMS nor NMR spectroscopy provided evidence for a derivative in which two molecules of 9EtG are coordinated to the ruthenium center, which may be prevented by steric hindrance.[60]

Cytotoxicity: The cytotoxicity of **1** and **4–6** (**2** and **3** are not sufficiently soluble for in vitro testing) was studied in human SW480 colon adenocarcinoma, CH1, A2780 and cisplatin-resistant A2780 ovarian carcinoma, A549 lung carcinoma, Me300 melanoma, LNZ308 glioblastoma, and HCEC endothelial cell lines by means of the MTT cell survival assay. Concentration–effect curves for CH1 and SW480 cells are depicted in Figure 9, and their IC_{50} values were determined after 96 h. Cytotoxicity of compounds **1**, **4**, and **5** towards the other cell lines are presented in Table 2 as IC_{50} values determined after 72 h of incubation.

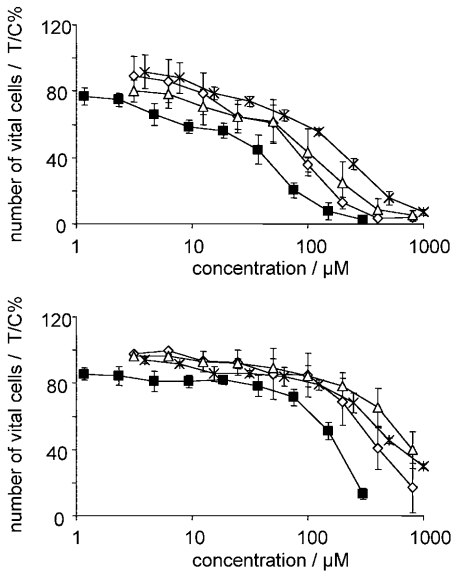

Figure 9. Concentration–effect curves of ruthenium complexes **1** and **4–6** after 96 h in CH1 (top) and SW480 (bottom) cells, obtained by the MTT assay. Values are means ± standard deviations from at least three independent experiments. **1**◇, **4**■, **5**△, **6**×.

Compound **4** showed the highest activity in all tested cell lines, but otherwise no structure–activity relationships with validity for all cell lines can be inferred from the data. The cytotoxicities of compounds **1**, **5**, and **6** are moderate with IC_{50} values in the range of 60–153 μM in the most sensitive cell line CH1. Other ruthenium drug candidates such as

Table 2. Cytotoxicity of ruthenium complexes **1** and **4–6** in terms of 50% inhibitory concentrations (IC_{50}) in human cancer and nontumorigenic cell lines after incubation for 72 or 96 h in the MTT assay. Values are means ± standard deviations, obtained from at least two independent experiments.

Compound	IC_{50} [μM]							
	Cancer cell lines							Nontumorigenic cells
	CH1[a]	SW480[a]	A2780[b]	CisR A2780[b]	LNZ308[b]	Me300[b]	A549[b]	HCEC[b]
1	60 ± 14	361 ± 122	504 ± 56	678 ± 80	575 ± 25	617 ± 13	498 ± 17	> 700
4	29 ± 4	150 ± 19	351 ± 89	374 ± 93	212 ± 54	327 ± 55	223 ± 14	506 ± 62
5	93 ± 26	500 ± 100	> 700	> 700	> 700	> 700	> 700	> 700
6	153 ± 13	430 ± 35	nd[c]	nd	nd	nd	nd	nd

[a] 96 h incubation. [b] 72 h incubation. [c] nd = not determined.

NAMI-A and certain RAPTA compounds exhibit similar cytotoxicities, and while they are much less active in vitro than, for example, cisplatin, they show excellent activities in vivo.[26,61] Interestingly, the comparable IC_{50} values found in A2780 and cisplatin-resistant A2780 cells suggest that these ruthenium complexes are not recognized by the same resistance mechanisms as cisplatin. Notably, the lowest activity was observed in nontumoral endothelial cells, and this indicates a selectivity towards cancer cells, in particular the CH1 cell lines with an order of magnitude difference in selectivity for **1** and **4**.

Conclusion

Ruthenium complexes with carbohydrate ligands resembling the structure of Ru(arene)(pta)-type complexes were prepared in order to evaluate the influence of the carbohydrate phosphite ligand on their in vitro anticancer activities. In water the phosphite ligand is hydrolyzed, and this process is activated by prior hydrolysis (of the chlorido ligand) at the ruthenium center. After dissolution in water the final hydrolysis product is a dimeric species. Hydrolysis of **1** was suppressed completely at high NaCl concentration, whereas hydrolysis in 4 mM NaCl was comparable to that in water. The complex resulting from hydrolysis of the Ru–Cl bonds and of the P–O bonds of the ligand were capable of binding to 9EtG with formation of 1:1 adducts. Complex **1** binds to both albumin and transferrin, but no conjugates with smaller proteins were observed.

In vitro anticancer activity tests revealed that the most lipophilic compound **4** is the most active. No correlation could be found with kinetics of hydrolysis, or other parameters.

The activity of the Ru complexes in the nontumorigenic cells was lower than in the tumor cell lines, which is an indication for a certain degree of selectivity towards malignant cells. The different behavior in cisplatin-resistant cells in comparison to the cisplatin-sensitive parental cell line suggests a different mode of action in comparison to the established platinum-based anticancer agents. However, in general sugar complexes based on platinum, titanium, and other metal complexes are not very active in vitro but were found to be sometimes more efficient in vivo than the established anticancer agents.[31,62]

Experimental Section

Materials: All reactions were carried out in dry solvents under an inert atmosphere in the dark. All chemicals obtained from commercial suppliers were used as received and were of analytical grade. $RuCl_3$ was obtained from Degussa (Germany) and sodium hydroxide and sodium dihydrogenphosphate from Fluka (Buchs, Switzerland). Disodium monohydrogenphosphate was purchased from Riedel-de Haen (Seelze, Germany). Human serum albumin (approximately 99%, Lot 111K7612), apotransferrin (97%, Lot 074K1370), and ammonium bicarbonate (purum, p.a.) were obtained from Sigma–Aldrich (Vienna, Austria). Cytochrome c and ubiquitin were purchased from Sigma. High-purity water was obtained from a Millipore Synergy 185 UV Ultrapure Water system (Molsheim, France). The dimer bis[dichlorido(η^6-*p*-cymene)ruthenium(II)][63] and the phosphorus sugar ligands[64–66] were synthesized by procedures reported previously. Complex formation was monitored by TLC with ethyl acetate as eluent.

^1H, ^{13}C, and ^{31}P NMR spectra were recorded by using a Bruker Avance DPX 400 instrument (Ultrashield Magnet) at $\tilde{\nu}$ = 400.13 (^1H), 100.63 (^{13}C), and 161.98 MHz (^{31}P) or a Bruker FT NMR spectrometer Avance III 500 MHz at $\tilde{\nu}$ = 500.10 (^1H), 125.75 (^{13}C), and 202.44 MHz (^{31}P) at 298 K. The 2D NMR spectra were measured in a gradient-enhanced mode.

An esquire3000 ion trap mass spectrometer (Bruker Daltonics, Bremen, Germany), equipped with an orthogonal ESI ion source, was used for MS measurements. The instrument was operated in positive-ion mode for characterizing proteins and protein–metal adducts. To ensure the best performance and to simulate physiological pH, samples containing varying drug-to-protein ratios (from 1:1 to 8:1) were incubated at 37 °C in 20 mM ammonium bicarbonate buffer adjusted to pH 7.4 by titration with 0.1 M formic acid. The samples were measured twice, after incubation periods of 30 min and 24 h. The solutions were introduced by flow injection at a rate of 4 μL min^{-1} by using a Cole-Parmer 74900 single-syringe infusion pump (Vernon Hills, IL). The ESIMS instrument was controlled by means of the esquireControl software (version 5.2), and all data were processed with DataAnalysis software (version 3.2), both from Bruker Daltonics.

Specific optical rotations were measured by using a Perkin–Elmer 341 polarimeter in a 10 cm cell at 20 °C. UV/Vis spectra were recorded by using a Perkin–Elmer Lambda 650 UV/Vis spectrometer in quartz cuvettes with 1 cm path length at 298 K in water from λ = 750 to 200 nm. Melting points were determined by means of a Büchi B-540 apparatus and are uncorrected. The elemental analyses were done by the Laboratory for Elemental Analysis, Faculty of Chemistry, University of Vienna, by using a Perkin–Elmer 2400 CHN Elemental Analyzer.

Hydrolysis: Samples were dissolved in H_2O/D_2O (9/1) at 25 °C. For investigating the effect of the chloride ion concentration on ligand exchange, sodium chloride was added to the solutions to set the chloride concentration from 0 to 100 mM.

Interaction with 9-ethylguanine: Complex **1** was incubated with 9EtG in H_2O at 25 °C in the dark at molar ratios of 1:1 and 2:1, and the time course of the reaction were determined. Before measuring NMR spectra 10 vol% D_2O was added.

Protein binding studies: CZE experiments were performed by using an HP^{3D} CE system (Agilent, Waldbronn, Germany) equipped with an on-column diode-array detector. For all measurements, uncoated fused-silica capillaries of 50 cm total length (50 μm i.d., 42 cm effective length) were used (Polymicro Technologies, Phoenix, AZ). Capillary and sample tray were thermostated at 37 °C. Injections were performed by applying a pressure of 50 mbar for 5 s (15 s in the case of **5**), and a constant voltage of 20 kV was used for all separations (the resulting current was about 30 μA). Detection was carried out at 200 nm. Prior to the first use, the capillary was flushed with 0.1 M HCl, water, 1 M NaOH, and again with water (10 min each) and then equilibrated with the background electrolyte (BGE) for 10 min. Before each injection, the capillary was purged with 0.1 M NaOH and water for 2 min each and finally conditioned with the BGE for 3 min.

The initial concentrations of protein and ruthenium complex in the 20 mM phosphate buffer (pH 7.4) sample mixtures were fixed for **1**, **5**, and **6** at 50 μM and 1 mM, respectively, and for **4**, owing to the low solubility of the complex, at 15 μM and 0.3 mM, and the samples were incubated at 37 °C. This constitutes a protein-to-drug ratio of 1:20, which is a reasonable approximation of a real situation shortly after intravenous administration. All solutions were passed through a 0.45 μm disposable membrane filter (Sartorius, Goettingen, Germany) before CZE analysis.

The rates of hydrolytic and protein-binding reactions were measured by monitoring the decrease in the peak area response due to the Ru complex anion. All rates were determined in 20 mM phosphate buffer as background electrolyte (pH 7.4) at 37 °C; the sample solutions were prepared as described above. The resulting ion strength was about 52 mM. For the determination of the rate constants k_{hyd} and k_{bind}, each kinetic series was repeated at least three times. Note that the kinetics of Ru–protein binding was assessed indirectly, because the peak of the adduct could not be separated from the protein peak, or selectively recorded by using the UV detection mode. Apparent binding rate constants were calculated by polynomial approximation of the rate constants of both processes, assuming first-order character of the binding reaction. In accordance with the kinetics theory of two parallel reactions,[67] the rate constant of the binding reaction can be expressed as a difference of the rate constants of the summative reaction, $k_{hyd+bind}$ and k_{hyd}: $k_{bind}=2k_{hyd+bind}-k_{hyd}$.

Crystallographic structure determination: X-ray diffraction measurements were performed on an APEXII CCD diffractometer at 296 (**1**) and 100 K (**2** and **3**). The single crystals were positioned 40 mm from the detector, and for **1** 2016 frames were measured, each for 60 s over 1°, whereas for **2** and **3** 1261 and 997 frames were recorded, each for 10 and 5 s over a 1° scan width (for **2** and **3**, respectively). The data were processed with the SAINT software package.[68] Crystal data, data collection parameters, and structure refinement details are given in Table S2 of the Supporting Information. The structures were solved by direct methods and refined by full-matrix least-squares techniques. Non-hydrogen atoms were refined with anisotropic displacement parameters. Hydrogen atoms were inserted at calculated positions and refined with a riding model. The following computer programs were used: structure solution, SHELXS-97;[69] refinement, SHELXL-97;[70] molecular diagrams, DS visualizer;[71] computer, Pentium IV; scattering factors.[72] CCDC 689442 (**1**), 689444 (**2**) and 689443 (**3**) contain the supplementary crystallographic data for this paper. These data can be obtained free of charge from The Cambridge Crystallographic Data Centre via www.ccdc.cam.ac.uk/data_request/cif.

Cell lines and culture conditions: CH1 cells originate from an ascites sample of a patient with a papillary cystadenocarcinoma of the ovary and were kindly provided by Lloyd R. Kelland, CRC Centre for Cancer Therapeutics, Institute of Cancer Research, Sutton, UK. SW480 colon adenocarcinoma and A549 lung carcinoma cells were obtained from the American Type Culture Collection (ATCC). Human Me300 melanoma cells were kindly provided by Dr D. Rimoldi, Ludwig Institute of Cancer Research, Lausanne branch, human cerebral endothelial cells (HCEC) by D. Staminirovic and A. Muruganandam, Ottawa, Canada, and LNZ308 glioblastoma cells by AC Diserens neurosurgery service, CHUV, Lausanne. All cell culture reagents were obtained from Iwaki or Gibco-BRL. Me300, A2780 and cisplatin-resistant A2780 cells were grown in RPMI 1640 medium, CH1 and SW480 cells in Minimal Essential Medium (MEM) plus 1 mM sodium pyruvate, 4 mM L-glutamine, and 1% nonessential amino acids (100×), and LNZ308, HCEC, and A549 cells in Dulbecco's Modified Eagle Medium (4.5 g L^{-1} glucose). All media were supplemented with 10% heat-inactivated fetal bovine serum and optionally with antibiotics. Cultures were maintained at 37 °C in a humidified atmosphere containing 5% CO_2.

Cytotoxicity tests in cancer cell lines: Cytotoxicity was determined by the MTT (3-(4,5-dimethyl-2-thiazolyl)-2,5-diphenyl-2*H*-tetrazolium bromide, Fluka) cell survival test, which measures the mitochondrial dehydrogenase activity of viable cells. CH1 and SW480 cells were harvested from culture flasks by trypsinization and seeded into 96-well microculture plates (Iwaki). Cell densities of 1.5×10^3 cells per well (CH1) and 2.5×10^3 cells per well (SW480) were chosen in order to ensure exponential growth throughout drug exposure. After a 24 h pre-incubation, cells were exposed for 96 h to solutions of the test compounds in complete culture medium. At the end of exposure, drug solutions were replaced by 100 μL per well of RPMI1640 culture medium supplemented with 10% heat-inactivated fetal bovine serum plus 20 μL per well of MTT solution in phosphate-buffered saline (5 mg mL^{-1}). After 4 h of incubation, the supernatants were removed, and the formazan crystals were dissolved in 150 μL DMSO per well. Optical densities at 550 nm were measured with a microplate reader (Tecan Spectra Classic), with a reference wavelength of $\lambda=690$ nm. Experiments were performed in sextuplicate wells and repeated at least twice.

The other cell lines were grown in 48-well cell culture plates (Corning, NY) until 20% confluence. Then culture medium was replaced with fresh medium containing the ruthenium complexes at concentrations varying from 0 to 500 μM, and cells were exposed to the complexes for 72 h. Cell survival was measured by using the MTT test with 2 h of incubation, then the cell culture supernatants were removed, the cell layers were dissolved in *i*PrOH/0.04 M HCl, and the absorbance at 540 nm was measured in a multiwell-plate reader (iEMS Reader MF, Labsystems, Bioconcept, Switzerland). Experiments were performed in triplicate wells and repeated at least twice. The number of viable cells was calculated as the ratio of the absorbance of treated to that of untreated cells, and IC_{50} values were calculated from dose–response curves.

Computational details: Full geometry optimization of all structures was carried out at the DFT level of theory using Becke's three-parameter hybrid exchange functional[73] in combination with the gradient-corrected correlation functional of Lee, Yang, and Parr[74] (B3LYP) with the help of the Gaussian 03[75] program package. Symmetry operations were not applied for all structures. The geometry optimization was carried out using a quasirelativistic Stuttgart pseudopotential describing 28 core electrons and the appropriate contracted basis set (8s7p6d)/[6s5p3d][76] for the ruthenium atom and the 6-31G(d) basis set for other atoms. The experimental X-ray structure of **1** (this work) was chosen as the starting geometry for the optimizations.

The Hessian matrix was calculated analytically for all optimized structures, to prove the location of correct minima (no imaginary frequencies) and to estimate the zero-point energy correction and thermodynamic parameters; the latter were calculated at 25 °C. The entropic terms and therefore the Gibbs free energies calculated by using the standard expressions for an ideal gas are over- or underestimated significantly for reactions occurring in solution in which a change in the number of molecules occurs. Hence, the ΔG values are not discussed in this work.

Solvent effects were taken into account in the single-point calculations based on the gas-phase equilibrium geometries by using the polarizable continuum model[77] in the CPCM version[78] with H_2O as a solvent and UAHF atomic radii. The enthalpies in solution H_s were estimated by addition of the solvation energy ΔG_{solv} to gas-phase enthalpies H_g. For accurate calculations of solvent effects, it is preferable to consider uncharged species. Hence, the full geometry optimization of cationic complexes **1a′** and **1b′** and of their hydrolysis products was performed with one or two chloride counterions, respectively (see Table S3 in the Supporting Information for the reaction energies and enthalpies for the gas phase and for

aqueous solutions, and Figure S6 for the equilibrium geometries of the calculated structures).

For the free phosphite ligand **L1**, two conformations were calculated (**La** and **Lb**, see Supporting Information). Only the most stable conformation **La** corresponding to the experimental structure[79] is discussed here. The equilibrium geometries and the main calculated bond lengths of **La** and **1′** are in reasonable agreement with the experimental X-ray structural data for **L1**[79] and **1** (this work). The maximum deviations of the theoretical and experimental parameters are 0.05 Å for the O1–C1 bond in **La** and Ru–C and P–O bonds in **1′**, and 0.03 Å for the C4–C5 bond in **1′**, whereas the differences for the other bonds do not exceed 0.02 Å and often fall within the 3σ interval of the X-ray data.

Dichlorido(η⁶-*p*-cymene)(3,5,6-bicyclophosphite-1,2-*O*-isopropylidene-α-D-glucofuranoside)ruthenium(II) (1): A solution of bis[dichlorido(η⁶-*p*-cymene)ruthenium(II)] (123 mg, 0.2 mmol) in dry CH_2Cl_2 (1 mL) was added to a solution of 3,5,6-bicyclophosphite-1,2-*O*-isopropylidene-α-D-glucofuranoside (100 mg, 0.4 mmol) in dry CH_2Cl_2 (20 mL). The mixture was stirred at 39 °C for 2 h. The solvent was then evaporated, and the residue washed with diethyl ether (3×5 mL) and dried under vacuum. Yield: 218 mg (98 %); m.p. 220–221 °C (decomp); $[\alpha]_D^{20}=25$ ($c=0.25$ in CH_2Cl_2); ^{1}H NMR (400.13 MHz, $CDCl_3$, 25 °C): $\delta=6.17$ (d, ^3J(H,H) = 3.5 Hz, 1H; H-1), 5.71 (d, ^3J(H,H) = 6.0 Hz, 1H; H-Ar), 5.69 (d, ^3J(H,H) = 6.0 Hz, 1H; H-Ar), 5.59 (d, ^3J(H,H) = 6.0 Hz, 1H; H-Ar), 5.55 (d, ^3J(H,H) = 6.0 Hz, 1H; H-Ar), 5.10 (m, 1H; H-5), 4.80 (m, 1H; H-3), 4.69 (d, ^3J(H,H) = 3.5 Hz, 1H; H-2), 4.45 (dd, ^2J (H,H) = 12.4 Hz, ^3J(H,P) = 9.4 Hz, 1H; H-6), 4.29 (m, 2H; H-6′, H-4), 2.91 (m, 1H; Ar-CH), 2.24 (s, 3H; Ar-CH_3), 1.52 (s, 3H; C(CH_3)$_2$), 1.36 (s, 3H; C(CH_3)$_2$), 1.28 (d, ^3J(H,H) = 6.6 Hz, 3H; Ar-C(CH_3)$_2$), 1.27 ppm (d, ^3J(H,H) = 6.6 Hz, 3H; Ar-CH(CH_3)$_2$); ^{13}C{^{1}H} NMR (100.63 MHz, $CDCl_3$, 25 °C): $\delta=113.0$ (*C*(CH_3)$_2$), 110.4 (C-Ar), 106.0 (C-1), 105.7 (C-Ar), 90.1 (C-Ar), 90.0 (C-Ar), 90.0 (C-Ar), 89.7 (C-Ar), 84.1 (d, ^3J(C,P) = 5.8 Hz; C-2), 79.3 (d, ^2J(C,P) = 8.7 Hz; C-3), 77.3 (d, ^3J(C,P) = 5.8 Hz; C-4), 74.9 (d, ^2J-(C,P) = 5.8 Hz; C-5), 69.4 (d, ^2J(C,P) = 9.7 Hz; C-6), 31.2 (*C*H(CH_3)$_2$-Ar), 27.3 (C(*C*H_3)$_2$), 26.6 (C(*C*H_3)$_2$), 22.6 (CH(*C*H_3)$_2$-Ar), 22.5 (CH(*C*H_3)$_2$-Ar), 19.1 ppm (*C*H_3-Ar); ^{31}P{^{1}H} NMR (161.98 MHz, $CDCl_3$, 25 °C): $\delta=$ 135.4 ppm; MS (ESI⁺): *m*/*z*: 519 [*M*−Cl]⁺, 577 [M+Na]⁺; elemental analysis calcd (%) for $C_{19}H_{27}Cl_2O_6PRu$: C 41.17, H 4.91; found: C 41.03, H 4.76.

Dibromido(η⁶-*p*-cymene)(3,5,6-bicyclophosphite-1,2-*O*-isopropylidene-α-D-glucofuranoside)ruthenium(II) (2): A solution of bis[dibromido(η⁶-*p*-cymene)ruthenium(II)] (196 mg, 0.25 mmol) in dry CH_2Cl_2 (1 mL) was added to a solution of 3,5,6-bicyclophosphite-1,2-*O*-isopropylidene-α-D-glucofuranoside (125 mg, 0.5 mmol) in dry CH_2Cl_2 (20 mL). The mixture was stirred at 39 °C for 2 h. The solvent was then evaporated, and the residue washed with diethyl ether (3×5 mL) and dried under vacuum. Yield: 297 mg (93 %); m.p. 224–225 °C (decomp); ^{1}H NMR (500.10 MHz, $CDCl_3$, 25 °C): $\delta=6.16$ (d, ^3J(H,H) = 3.5 Hz, 1H; H-1), 5.70 (d, ^3J(H,H) = 6.1 Hz, 1H; H-Ar), 5.57 (d, ^3J(H,H) = 5.0 Hz, 1H; H-Ar), 5.56 (d, ^3J-(H,H) = 5.0 Hz, 1H; H-Ar), 5.10 (m, 1H; H-5), 4.79 (m, 1H; H-3), 4.68 (d, ^3J(H,H) = 3.5 Hz, 1H; H-2), 4.43 (dd, ^2J(H,H) = 12.6, ^3J(H,P) = 7.3 Hz, 1H; H-6), 4.29 (m, 2H; H-6′, H-4), 3.02 (m, 1H; Ar-CH), 2.36 (s, 3H; Ar-CH_3), 1.51 (s, 3H; C(CH_3)$_2$), 1.36 (s, 3H; C(CH_3)$_2$), 1.29 (d, ^3J(H,H) = 6.8 Hz, 3H; Ar-CH(CH_3)$_2$), 1.28 ppm (d, ^3J(H,H) = 6.3 Hz, 3H; Ar-CH-(*C*H_3)$_2$); ^{13}C{^{1}H} NMR (125.75 MHz, $CDCl_3$, 25 °C): $\delta=112.6$ (*C*(CH_3)$_2$), 111.7 (C-Ar), 105.6 (C-1), 105.4 (C-Ar), 89.5 (C-Ar), 89.4 (C-Ar), 89.1 (C-Ar), 83.7 (d, ^3J(C,P) = 6.2 Hz; C-2), 79.1 (d, ^2J(C,P) = 7.0 Hz; C-3), 76.8 (d, ^3J(C,P) = 4.0 Hz; C-4), 74.6 (d, ^2J(C,P) = 4.0 Hz; C-5), 69.2 (d, ^2J-(C,P) = 7.0 Hz, C-6), 31.2 (Ar-*C*H(CH_3)$_2$), 26.9 (C(*C*H_3)$_2$), 26.3 (C-(*C*H_3)$_2$), 22.4 (Ar-CH(*C*H_3)$_2$), 22.3 (Ar-CH(*C*H_3)$_2$), 19.4 ppm (Ar-CH_3); ^{31}P{^{1}H} NMR (202.44 MHz, $CDCl_3$, 25 °C): $\delta=133.5$ ppm; MS (ESI⁺): *m*/*z*: 667 [*M*+Na]⁺; elemental analysis calcd (%) for $C_{19}H_{27}Br_2O_6PRu$: C 35.48, H 4.23; found: C 35.62, H 4.10.

Diiodido(η⁶-*p*-cymene)(3,5,6-bicyclophosphite-1,2-*O*-isopropylidene-α-D-glucofuranoside)ruthenium(II) (3): A solution of bis[diiodido(η⁶-*p*-cymene)ruthenium] (244 mg, 0.25 mmol) in dry CH_2Cl_2 (1 mL) was added to a solution of 3,5,6-bicyclophosphite-1,2-*O*-isopropylidene-α-D-glucofuranoside (125 mg, 0.5 mmol) in dry CH_2Cl_2 (20 mL). The mixture was stirred at 39 °C for 2 h. The solvent was then evaporated, and the residue washed with diethyl ether (3×5 mL) and dried under vacuum. Yield: 334 mg (91 %); m.p. 244–245 °C (decomp); ^{1}H NMR (500.10 MHz, $CDCl_3$, 25 °C): $\delta=6.15$ (d, ^3J(H,H) = 3.5 Hz, 1H; H-1), 5.74 (d, ^3J(H,H) = 6.5 Hz, 1H; H-Ar), 5.72 (d, ^3J(H,H) = 6.5 Hz, 1H; H-Ar), 5.60 (d, ^3J-(H,H) = 5.5 Hz, 1H; H-Ar), 5.55 (d, ^3J(H,H) = 5.5 Hz, 1H; H-Ar), 5.10 (m, 1H; H-5), 4.77 (m, 1H; H-3), 4.67 (d, ^3J(H,H) = 3.2 Hz, 1H; H-2), 4.37 (dd, ^2J(H,H) = 12.9 Hz, ^3J(H,P) = 7.5 Hz, 1H; H-6), 4.26 (m, 2H; H-6′, H-4), 3.22 (m, 1H; H-Ar), 2.54 (s, 3H; CH_3-Ar), 1.52 (s, 3H; C-(CH_3)$_2$), 1.37 (s, 3H; C(CH_3)$_2$), 1.32 (d, ^3J(H,H) = 6.9 Hz, 3H; C(CH_3)$_2$-Ar), 1.30 ppm (d, ^3J(H,H) = 6.9 Hz, 3H; CH(CH_3)$_2$-Ar); ^{13}C{^{1}H} NMR (125.75 MHz, $CDCl_3$, 25 °C): $\delta=112.7$ (*C*(CH_3)$_2$), 112.1 (C-Ar), 105.7 (C-1), 105.6 (C-Ar), 90.6 (C-Ar), 90.3 (C-Ar), 90.1 (C-Ar), 89.8 (C-Ar), 83.9 (d, ^3J(C,P) = 6.4 Hz; C-2), 79.1 (d, ^2J(C,P) = 8.2 Hz; C-3), 76.8 (d, ^3J-(C,P) = 4.6 Hz; C-4), 74.8 (d, ^2J(C,P) = 4.6 Hz; C-5), 69.2 (d, ^3J(C,P) = 9.1 Hz; C-6), 31.9 (Ar-*C*H(CH_3)$_2$), 29.7 (C(CH_3)$_2$), 26.9 (C(*C*H_3)$_2$), 26.2 (C(*C*H_3)$_2$), 22.8 (Ar-CH(*C*H_3)$_2$), 22.7 (Ar-CH(*C*H_3)$_2$), 20.5 ppm (Ar-CH_3); ^{31}P{^{1}H} NMR (202.44 MHz, $CDCl_3$, 25 °C): $\delta=136.2$ ppm; MS (ESI⁺): *m*/*z*: 761 [*M*+Na]⁺; elemental analysis calcd (%) for $C_{19}H_{27}I_2O_6PRu$: C 30.95, H 3.69.; found: C 31.05, H 3.54.

Dichlorido(η⁶-*p*-cymene)(3,5,6-bicyclophosphite-1,2-*O*-cyclohexylidene-α-D-glucofuranoside)ruthenium(II) (4): A solution of bis[dichlorido(η⁶-*p*-cymene)ruthenium(II)] (202 mg, 0.3 mmol) in CH_2Cl_2 (2 mL) was added to a solution of 3,5,6-bicyclophosphite-1,2-*O*-cyclohexylidene-α-D-glucofuranoside (173 mg, 0.6 mmol) in CH_2Cl_2 (40 mL). The mixture was stirred at 39 °C for 2 h. The solvent was then evaporated, and the residue washed with diethyl ether (3×5 mL) and dried under vacuum. Yield: 367 mg (98 %); m.p. 160–161 °C (decomp), $[\alpha]_D^{20}=30$ ($c=0.25$ in CH_2Cl_2); ^{1}H NMR (400.13 MHz, $CDCl_3$, 25 °C): $\delta=6.17$ (d, ^3J(H,H) = 3.5 Hz, 1H; H-1), 5.70 (d, ^3J(H,H) = 6.0 Hz, 1H; H-Ar), 5.68 (d, ^3J(H,H) = 6.2 Hz, 1H; H-Ar), 5.60 (d, ^3J(H,H) = 5.9 Hz, 1H; H-Ar), 5.56 (d, ^3J(H,H) = 5.9 Hz, 1H; H-Ar), 5.08 (m, 1H; H-5), 4.81 (m, 1H; H-3), 4.68 (d, ^3J-(H,H) = 3.5 Hz, 1H, H-2), 4.45 (dd, ^2J(H,H) = 12.4 Hz, ^3J(H,P) = 9.3 Hz, 1H; H-6), 4.29 (m, 2H; H-6′, H-4), 2.91 (m, 1H; H-Ar), 2.25 (s, 3H; Ar-CH_3), 1.64 (m, 8H; C_6H_{10}), 1.41 (m, 2H; C_6H_{10}), 1.28 (s, 3H; Ar-CH-(CH_3)$_2$), 1.26 ppm (s, 3H; Ar-CH(CH_3)$_2$); ^{13}C{^{1}H} NMR (100.63 MHz, $CDCl_3$, 25 °C): $\delta=114.1$ (*C*(CH_3)$_2$), 112.6 (C-Ar), 105.9 (C-Ar), 105.6 (C-1), 90.2 (C-Ar), 89.9 (C-Ar), 89.8 (C-Ar), 89.7 (C-Ar), 83.7 (d, ^3J(C,P) = 6.1 Hz; C-2), 79.3 (d, ^2J(C,P) = 10.5 Hz; C-3), 77.5 (d, ^3J(C,P) = 6.0 Hz; C-4), 74.7 (d, ^2J(C,P) = 6.1 Hz; C-5), 69.2 (d, ^2J(C,P) = 9.6 Hz; C-6), 31.2 (*C*H(CH_3)$_2$-Ar), 27.3 (C(*C*H_3)$_2$), 26.6 (C(*C*H_3)$_2$), 22.6 (CH(*C*H_3)$_2$-Ar), 22.5 (CH(*C*H_3)$_2$-Ar), 19.1 ppm (*C*H_3-Ar); ^{31}P{^{1}H} NMR (161.98 MHz, $CDCl_3$, 25 °C): $\delta=135.4$ ppm; MS (ESI⁺): *m*/*z*: 617 [*M*+Na]⁺; elemental analysis calcd (%) for $C_{22}H_{31}Cl_2O_6PRu$: C 44.45, H 5.26; found: C 44.31, H 5.23.

Dichlorido(η⁶-*p*-cymene)(3,5,6-bicyclophosphite-ethyl-1-thio-α-D-glucofuranoside)ruthenium(II) (5): A solution of bis[dichlorido(η⁶-*p*-cymene) ruthenium(II)] (185 mg, 0.3 mmol) in CH_2Cl_2 (2 mL) was added to a solution of 3,5,6-bicyclophosphite-1-thio-α-D-glucofuranoside (153 mg, 0.6 mmol) in CH_2Cl_2 (40 mL). The mixture was stirred at 39 °C for 2 h. The solvent was evaporated, and the residue washed with diethyl ether (3×5 mL) and dried under vacuum. Yield: 331 mg (98 %); m.p. 175–176 °C (decomp); $[\alpha]_D^{20}=5$ ($c=0.25$ in CH_2Cl_2); ^{1}H NMR (400.13 MHz, $CDCl_3$, 25 °C): $\delta=5.71$ (d, ^3J(H,H) = 5.8 Hz, 1H; H-Ar), 5.64 (d, ^3J-(H,H) = 2.8 Hz, 1H; H-1), 5.61 (d, ^3J(H,H) = 5.8, 1H; H-Ar), 5.55 (d, ^3J-(H,H) = 5.6 Hz, 1H; H-Ar), 5.07 (m, 1H; H-5), 4.89 (s, 1H; H-3), 4.54 (t, ^2J(H,H), ^3J(H,P) = 10.0 Hz, 1H; H-6), 4.47–4.42 (m, 2H; H-4, H-2), 4.28 (m, 1H; H-6′), 2.89 (m, 1H; Ar-CH), 2.77 (m, 2H; CH_2CH$_3$), 2.23 (s, 3H; Ar-CH_3), 1.36 (t, ^3J(H,H) = 7.6 Hz, 3H; CH_2CH_3), 1.27 (s, 3H; Ar-CH(CH_3)$_2$), 1.25 (s, 3H; Ar-CH(CH_3)$_2$); ^{13}C{^{1}H} NMR (100.63 MHz, $CDCl_3$, 25 °C): $\delta=110.0$ (C-Ar), 106.0 (C-Ar), 90.5 (C-Ar), 90.2 (C-1), 90.1 (C-Ar), 89.5 (C-Ar), 81.3 (d, ^2J(C,P) = 7.8 Hz, C-3), 77.7 (C-4, C-2), 75.6 (d, ^2J(C,P) = 4.9 Hz, C-5), 69.1 (d, ^2J(C,P) = 6.8 Hz, C-6), 31.3 (Ar-*C*H(CH_3)$_2$), 26.1 (S*C*H_2CH$_3$), 22.5 (Ar-CH(*C*H_3)$_2$), 19.1 (Ar-CH_3), 15.8 ppm (SCH$_2$*C*H_3); ^{31}P{^{1}H} NMR (161.98 MHz, $CDCl_3$, 25 °C): $\delta=$ 134.6 ppm; MS (ESI⁺): *m*/*z*: 581 [*M*+Na]⁺; elemental analysis calcd (%) for $C_{18}H_{27}Cl_2O_5PRuS$: C 38.72, H 4.87; found: C 39.00, H 4.73.

Dichlorido(η⁶-*p*-cymene)(3,5,6-bicyclophosphite-*N*-acetyl-α-D-glucofuranosylamine)ruthenium(II) (6): A solution of bis[dichlorido(η⁶-*p*-cyme-

ne)ruthenium(II)] (66 mg, 0.11 mmol) in CH_2Cl_2 (2 mL) was added to a solution of 3,5,6-bicyclophosphite-*N*-acetyl-α-D-glucofuranosylamine (54 mg, 0.22 mmol) in CH_2Cl_2 (40 mL). The mixture was stirred at room temperature for 12 h. The solvent was evaporated, and the residue washed with diethyl ether (3×5 mL) and dried under vacuum at 60 °C. Yield: 117 mg (97 %); m.p. 205–206 °C (decomp); $[\alpha]_D^{20}=14$ ($c=0.25$ in CH_2Cl_2); ^{1}H NMR (400.13 MHz, $CDCl_3$, 25 °C): $\delta=6.98$ (d, ^3J(H,H)= 9.1 Hz, 1H; NH), 6.12 (dd, ^3J(H,H)=9.3 Hz, ^3J(H,H)=4.1 Hz, 1H; H-1), 5.74 (d, ^3J(H,H)=6.3 Hz, 1H; H-Ar), 5.72 (d, ^3J(H,H)=6.3 Hz, 1H; H-Ar), 5.62 (d, ^3J(H,H)=6.2, 1H; H-Ar), 5.60 (d, ^3J(H,H)=6.2, 1H; H-Ar), 5.09 (m, 1H; H-5), 4.95 (s, 1H; H-3), 4.61 (t, ^2J(H,H), ^3J(H,P)= 8.9 Hz, 1H; H-6), 4.50 (s, 1H; H-4), 4.29 (m, 1H; H-2), 4.20 (m, 1H; H-6′), 2.86 (m, 1H; Ar-CH), 2.20 (s, 3H; Ar-CH_3), 2.09 (s, 3H; NHCOCH_3), 1.26 (s, 3H; Ar-CH(CH_3)$_2$), 1.25 ppm (s, 3H; Ar-CH(CH_3)$_2$); ^{13}C{^{1}H} NMR (100.63 MHz, $CDCl_3$, 25 °C): $\delta=171.6$ (NH*C*OCH$_3$), 110.1 (C-Ar), 105.6 (C-Ar), 90.2 (C-Ar), 89.8 (C-Ar), 89.7 (C-Ar), 82.3 (C-1), 81.2 (d, ^2J(C,P)=8.0 Hz; C-3), 76.3 (d, ^3J(C,P)= 5.2 Hz; C-4), 76.0 (d, ^2J(C,P)=5.6 Hz; C-5), 74.2 (C-2), 69.2 (d, ^2J(C,P)= 9.0 Hz; C-6), 31.1 (Ar-*C*H(CH$_3$)$_2$), 23.9 (NHCO*C*H$_3$), 22.3 (Ar-CH(*C*H$_3$)$_2$), 19.0 ppm (Ar-CH$_3$); ^{31}P{^{1}H} NMR (161.98 MHz, $CDCl_3$, 25 °C): $\delta=134.5$ ppm; MS (ESI$^+$): *m*/*z*: 578 $[M+Na]^+$; elemental analysis calcd (%) for $C_{18}H_{26}Cl_2NO_6PRu$: C 38.93, H 4.72; N 2.52; found: C 38.67, H 4.78, N 2.71.

Acknowledgements

The authors are indebted to the FFG—Austrian Research Promotion Agency (811591), the Austrian Council for Research and Technology Development (IS526001), the FWF—Austrian Science Fund (P16186-NO3, P18123-N11, P16192-NO3; C.G.H. Schrödinger Fellowship J2613-N19), the Higher Education Commission of Pakistan (M.H.), the Austrian Exchange Service, the Swiss National Science Foundation (individual short visit A.A.N., No. 120985) and COST D20 and D39. This research was supported by a Marie Curie Intra European Fellowship within the 7th European Community Framework Program project 220890-SuRuCo-(A.A.N.). M.L.K. is grateful to the Fundação para a Ciência e a Tecnologia (FCT) and Instituto Superior Técnico (IST) for the contract within the Ciência 2007 program. The authors thank the computer center of the University of Vienna for technical support and computer time at the Linux-PC cluster Schroedinger III, and Alexander Roller for collecting the X-ray data.

[1] C. S. Allardyce, A. Dorcier, C. Scolaro, P. J. Dyson, *Appl. Organomet. Chem.* **2005**, *19*, 1–10.
[2] G. Jaouen, *Bioorganometallics*, Wiley-VCH, Weinheim, **2006**.
[3] C. G. Hartinger, P. J. Dyson, *Chem. Soc. Rev.* **2008**, in press.
[4] B. Rosenberg, L. VanCamp, J. E. Trosko, V. H. Mansour, *Nature* **1969**, *222*, 385–386.
[5] P. Köpf-Maier, *Eur. J. Clin. Pharmacol.* **1994**, *47*, 1–16.
[6] C. G. Hartinger, S. Zorbas-Seifried, M. A. Jakupec, B. Kynast, H. Zorbas, B. K. Keppler, *J. Inorg. Biochem.* **2006**, *100*, 891–904.
[7] J. M. Rademaker-Lakhai, D. van den Bongard, D. Pluim, J. H. Beijnen, J. H. Schellens, *Clin. Cancer Res.* **2004**, *10*, 3717–3727.
[8] C. G. Hartinger, M. A. Jakupec, S. Zorbas-Seifried, M. Groessl, A. Egger, W. Berger, H. Zorbas, P. J. Dyson, B. K. Keppler, *Chem. Biodiversity* **2008**, in press.
[9] M. Pongratz, P. Schluga, M. A. Jakupec, V. B. Arion, C. G. Hartinger, G. Allmaier, B. K. Keppler, *J. Anal. At. Spectrom.* **2004**, *19*, 46–51.
[10] M. Sulyok, S. Hann, C. G. Hartinger, B. K. Keppler, G. Stingeder, G. Koellensperger, *J. Anal. At. Spectrom.* **2005**, *20*, 856–863.
[11] A. R. Timerbaev, C. G. Hartinger, S. S. Aleksenko, B. K. Keppler, *Chem. Rev.* **2006**, *106*, 2224–2248.
[12] M. Groessl, C. G. Hartinger, K. Polec-Pawlak, M. Jarosz, B. K. Keppler, *Electrophoresis* **2008**, *29*, 2224–2232.
[13] M. Groessl, E. Reisner, C. G. Hartinger, R. Eichinger, O. Semenova, A. R. Timerbaev, M. A. Jakupec, V. B. Arion, B. K. Keppler, *J. Med. Chem.* **2007**, *50*, 2185–2193.
[14] P. Schluga, C. G. Hartinger, A. Egger, E. Reisner, M. Galanski, M. A. Jakupec, B. K. Keppler, *Dalton Trans.* **2006**, 1796–1802.
[15] A. Egger, V. B. Arion, E. Reisner, B. Cebrian-Losantos, S. Shova, G. Trettenhahn, B. K. Keppler, *Inorg. Chem.* **2005**, *44*, 122–132.
[16] R. H. Grubbs, *Handbook of Metathesis, Vol. 2*, Wiley-VCH, Weinheim, **2003**.
[17] S.-I. Murahashi, *Ruthenium in Organic Synthesis*, Wiley-VCH, Weinheim, **2005**.
[18] C. Fellay, J. Dyson Paul, G. Laurenczy, *Angew. Chem.* **2008**, *120*, 4030–4032; *Angew. Chem. Int. Ed.* **2008**, *47*, 3966–3968.
[19] Y. K. Yan, M. Melchart, A. Habtemariam, P. J. Sadler, *Chem. Commun.* **2005**, 4764–4776.
[20] P. J. Dyson, G. Sava, *Dalton Trans.* **2006**, 1929–1933.
[21] W. H. Ang, P. J. Dyson, *Eur. J. Inorg. Chem.* **2006**, 4003–4018.
[22] W. F. Schmid, R. O. John, V. B. Arion, M. A. Jakupec, B. K. Keppler, *Organometallics* **2007**, *26*, 6643–6652.
[23] W. F. Schmid, R. O. John, G. Muehlgassner, P. Heffeter, M. A. Jakupec, M. Galanski, W. Berger, V. B. Arion, B. K. Keppler, *J. Med. Chem.* **2007**, *50*, 6343–6355.
[24] M. G. Mendoza-Ferri, C. G. Hartinger, A. A. Nazarov, W. Kandioller, K. Severin, B. K. Keppler, *Appl. Organomet. Chem.* **2008**, *22*, 326–332.
[25] M. G. Mendoza-Ferri, C. G. Hartinger, R. E. Eichinger, N. Stolyarova, K. Severin, M. A. Jakupec, A. A. Nazarov, B. K. Keppler, *Organometallics* **2008**, *27*, 2405–2407.
[26] C. Scolaro, A. Bergamo, L. Brescacin, R. Delfino, M. Cocchietto, G. Laurenczy, T. J. Geldbach, G. Sava, P. J. Dyson, *J. Med. Chem.* **2005**, *48*, 4161–4171.
[27] P. J. Dyson, *Chimia* **2007**, *61*, 698–703.
[28] E. E. Nifantyev, M. P. Koroteev, A. M. Koroteev, V. K. Belsky, A. I. Stash, M. Y. Antipin, K. A. Lysenko, L. Cao, *J. Organomet. Chem.* **1999**, *587*, 18–27.
[29] A. M. Koroteev, A. T. Teleshov, M. P. Koroteev, E. E. Nifant'ev, *Russ. J. Gen. Chem.* **2004**, *74*, 1313–1316.
[30] A. A. Nazarov, M. P. Koroteev, C. G. Hartinger, B. K. Keppler, E. E. Nifant'ev, *Monatsh. Chem.* **2005**, *136*, 137–146.
[31] C. G. Hartinger, A. A. Nazarov, S. M. Ashraf, P. J. Dyson, B. K. Keppler, *Curr. Med. Chem.* **2008**, in press.
[32] A. F. A. Peacock, M. Melchart, R. J. Deeth, A. Habtemariam, S. Parsons, P. J. Sadler, *Chem. Eur. J.* **2007**, *13*, 2601–2613.
[33] C. S. Allardyce, P. J. Dyson, D. J. Ellis, S. L. Heath, *Chem. Commun.* **2001**, 1396–1397.
[34] A. Dorcier, P. J. Dyson, C. Gossens, U. Rothlisberger, R. Scopelliti, I. Tavernelli, *Organometallics* **2005**, *24*, 2114–2123.
[35] B. Kure, S. Ogo, D. Inoki, H. Nakai, K. Isobe, S. Fukuzumi, *J. Am. Chem. Soc.* **2005**, *127*, 14366–14374.
[36] E. Hodson, S. J. Simpson, *Polyhedron* **2004**, *23*, 2695–2707.
[37] E. Nifant'ev, M. Koroteev, E. Grigory'ev, V. Belsky, CSD version 5.28 (November 2006), refcode TAJNAU, personal communication, **2003**.
[38] B. Cebrián-Losantos, E. Reisner, C. R. Kowol, A. Roller, S. Shova, V. B. Arion, B. K. Keppler, *Inorg. Chem.* **2008**, *47*, 6513–6523.
[39] C. Scolaro, C. G. Hartinger, C. S. Allardyce, B. K. Keppler, P. J. Dyson, *J. Inorg. Biochem*. **2008**, DOI: 10.1016/j.jinorgbio. 2008.05.004.
[40] E. E. Nifant'ev, M. P. Koroteev, N. M. Pugashova, A. R. Bekker, V. K. Bel'skii, N. S. Magomedova, A. M. Il′inets, *Zh. Obshch. Khim.* **1990**, *60*, 1412–1419.
[41] N. S. Magomedova, A. N. Sobolev, V. K. Bel'skii, M. P. Koroteev, N. M. Pugashova, E. E. Nifant'ev, *Phosphorus Sulfur Silicon Relat. Elem.* **1991**, *57*, 261–271.
[42] E. Pacsu, E. J. Wilson, Jr., *J. Am. Chem. Soc.* **1939**, *61*, 1450–1454.
[43] A. R. Timerbaev, S. S. Aleksenko, K. Polec-Pawlak, R. Ruzik, O. Semenova, C. G. Hartinger, S. Oszwaldowski, M. Galanski, M. Jarosz, B. K. Keppler, *Electrophoresis* **2004**, *25*, 1988–1995.

[44] C. G. Hartinger, S. Hann, G. Koellensperger, M. Sulyok, M. Groessl, A. R. Timerbaev, A. V. Rudnev, G. Stingeder, B. K. Keppler, *Int. J. Clin. Pharmacol. Ther.* **2005**, *43*, 583–585.
[45] A. V. Rudnev, S. S. Aleksenko, O. Semenova, C. G. Hartinger, A. R. Timerbaev, B. K. Keppler, *J. Sep. Sci.* **2005**, *28*, 121–127.
[46] A. R. Timerbaev, A. V. Rudnev, O. Semenova, C. G. Hartinger, B. K. Keppler, *Anal. Biochem.* **2005**, *341*, 326–333.
[47] K. Polec-Pawlak, J. K. Abramski, O. Semenova, C. G. Hartinger, A. R. Timerbaev, B. K. Keppler, M. Jarosz, *Electrophoresis* **2006**, *27*, 1128–1135.
[48] A. R. Timerbaev, C. G. Hartinger, B. K. Keppler, *TrAC Trends Anal. Chem.* **2006**, *25*, 868–875.
[49] S. S. Aleksenko, C. G. Hartinger, O. Semenova, K. Meelich, A. R. Timerbaev, B. K. Keppler, *J. Chromatogr. A* **2007**, *1155*, 218–221.
[50] C. G. Hartinger, W. H. Ang, A. Casini, L. Messori, B. K. Keppler, P. J. Dyson, *J. Anal. At. Spectrom.* **2007**, *22*, 960–967.
[51] C. G. Hartinger, B. K. Keppler, *Electrophoresis* **2007**, *28*, 3436–3446.
[52] C. G. Hartinger, Y. O. Tsybin, J. Fuchser, P. J. Dyson, *Inorg. Chem.* **2008**, *47*, 17–19.
[53] M. Ravera, S. Baracco, C. Cassino, D. Colangelo, G. Bagni, G. Sava, D. Osella, *J. Inorg. Biochem.* **2004**, *98*, 984–990.
[54] R. Feng, Y. Konishi, A. W. Bell, *J. Am. Soc. Mass Spectrom.* **1991**, *2*, 387–401.
[55] U. Warnke, C. Rappel, H. Meier, C. Kloft, M. Galanski, C. G. Hartinger, B. K. Keppler, U. Jaehde, *ChemBioChem* **2004**, *5*, 1543–1549.
[56] C. G. Hartinger, A. R. Timerbaev, B. K. Keppler, *Electrophoresis* **2003**, *24*, 2023–2037.
[57] H.-K. Liu, S. J. Berners-Price, F. Wang, J. A. Parkinson, J. Xu, J. Bella, P. J. Sadler, *Angew. Chem.* **2006**, *118*, 8333–8336; *Angew. Chem. Int. Ed.* **2006**, *45*, 8153–8156.
[58] S. Zorbas-Seifried, C. G. Hartinger, K. Meelich, M. Galanski, B. K. Keppler, H. Zorbas, *Biochemistry* **2006**, *45*, 14817–14825.
[59] S. Zorbas-Seifried, M. A. Jakupec, N. V. Kukushkin, M. Grössl, C. G. Hartinger, O. Semenova, H. Zorbas, V. Y. Kukushkin, B. K. Keppler, *Mol. Pharmacol.* **2007**, *71*, 357–365.
[60] A. Dorcier, C. G. Hartinger, R. Scopelliti, R. H. Fish, B. K. Keppler, P. J. Dyson, *J. Inorg. Biochem.* **2008**, *102*, 1066–1076.
[61] E. Alessio, G. Mestroni, A. Bergamo, G. Sava, *Curr. Top. Med. Chem.* **2004**, *4*, 1525–1535.
[62] I. Berger, A. A. Nazarov, C. G. Hartinger, M. Groessl, S.-M. Valiahdi, M. A. Jakupec, B. K. Keppler, *ChemMedChem* **2007**, *2*, 505–514.
[63] M. A. Bennett, T. N. Huang, T. W. Matheson, A. K. Smith, *Inorg. Synth.* **1982**, *21*, 74–78.
[64] N. K. Kochetkov, E. E. Nifant'ev, M. P. Koroteev, Z. K. Zhane, A. A. Borisenko, *Carbohydr. Res.* **1976**, *47*, 221–231.
[65] E. E. Nifant'ev, M. P. Koroteev, A. A. Nazarov, *Dokl. Akad. Nauk SSSR* **1998**, *363*, 76–78.
[66] A. A. Nazarov, M. P. Koroteev, C. G. Hartinger, B. K. Keppler, E. E. Nifant'ev, *Tetrahedron* **2005**, *61*, 10943–10950.
[67] A. G. Sykes, *Kinetics of Inorganic Reactions*, Pergamon Press, London, **1966**.
[68] M. R. Pressprich, J. Chambers, SAINT + Integration Engine, Program for Crystal Structure Integration, Bruker Analytical X-ray systems, Madison, **2004**.
[69] G. M. Sheldrick, SHELXS-97, Program for Crystal Structure Solution, University Göttingen (Germany), **1997**.
[70] G. M. Sheldrick, SHELXL-97, Program for Crystal Structure Refinement, University Göttingen (Germany), **1997**.
[71] DS Visualizer 2.0, Accelrys Software Inc., San Diego, **2007**.
[72] *International Tables for X-ray Crystallography, Vol. C*, Kluwer Academic Press, Dordrecht, The Netherlands, **1992**.
[73] A. D. Becke, *J. Chem. Phys.* **1993**, *98*, 5648–5652.
[74] C. Lee, W. Yang, R. G. Parr, *Phys. Rev. B* **1988**, *37*, 785–789.
[75] Gaussian 03, Revision D.01, M. J. Frisch, G. W. Trucks, H. B. Schlegel, G. E. Scuseria, M. A. Robb, J. R. Cheeseman, J. Montgomery, J. A., T. Vreven, K. N. Kudin, J. C. Burant, J. M. Millam, S. S. Iyengar, J. Tomasi, V. Barone, B. Mennucci, M. Cossi, G. Scalmani, N. Rega, G. A. Petersson, H. Nakatsuji, M. Hada, M. Ehara, K. Toyota, R. Fukuda, J. Hasegawa, M. Ishida, T. Nakajima, Y. Honda, O. Kitao, H. Nakai, M. Klene, X. Li, J. E. Knox, H. P. Hratchian, J. B. Cross, V. Bakken, C. Adamo, J. Jaramillo, R. Gomperts, R. E. Stratmann, O. Yazyev, A. J. Austin, R. Cammi, C. Pomelli, J. W. Ochterski, P. Y. Ayala, K. Morokuma, G. A. Voth, P. Salvador, J. J. Dannenberg, V. G. Zakrzewski, S. Dapprich, A. D. Daniels, M. C. Strain, O. Farkas, D. K. Malick, A. D. Rabuck, K. Raghavachari, J. B. Foresman, J. V. Ortiz, Q. Cui, A. G. Baboul, S. Clifford, J. Cioslowski, B. B. Stefanov, G. Liu, A. Liashenko, P. Piskorz, I. Komaromi, R. L. Martin, D. J. Fox, T. Keith, M. A. Al-Laham, C. Y. Peng, A. Nanayakkara, M. Challacombe, P. M. W. Gill, B. Johnson, W. Chen, M. W. Wong, C. Gonzalez, J. A. Pople, Gaussian, Inc., Wallingford, **2004**.
[76] D. Andrae, U. Haeussermann, M. Dolg, H. Stoll, H. Preuss, *Theor. Chim. Acta* **1990**, *77*, 123–141.
[77] J. Tomasi, M. Persico, *Chem. Rev.* **1994**, *94*, 2027–2094.
[78] V. Barone, M. Cossi, *J. Phys. Chem. A* **1998**, *102*, 1995–2001.
[79] L. A. Aslanov, S. S. Sotman, V. B. Rybakov, V. I. Andrianov, Z. S. Safina, M. P. Koroteev, E. E. Nifant'ev, *Zh. Strukt. Khim.* **1979**, *20*, 1125–1127.

Received: May 28, 2008
Published online: August 8, 2008

